

***Germes* is involved in translocation of germ plasm during development of *Xenopus* primordial germ cells**

TAKESHI YAMAGUCHI*, AYAKA TAGUCHI, KENJI WATANABE and HIDEFUMI ORII*

Department of Life Science, University of Hyogo, Kamigori, Akou-gun, Hyogo, Japan

ABSTRACT *Germes* mRNA and protein are components of the germ plasm in *Xenopus laevis*. Previously, based on phenotypic observations of tailbud embryos expressing intact and mutant *Germes*, it was suggested that *Germes* is involved in the organization of germ plasm (Berekelya *et al.*, 2007). Recently, to observe the germ plasm in a living embryo, we generated transgenic *Xenopus* expressing EGFP fused with a mitochondrial targeting signal, because germ plasm is enriched with mitochondria (Taguchi *et al.*, 2012). Using this transgenic *Xenopus*, we demonstrate that *Germes* plays an essential role in the translocation of germ plasm from the cortex to the perinuclear region in primordial germ cells during early gastrulation.

KEY WORDS: PGC, germline, *DEADSouth*, mitochondrial cloud, chromatoid body

In early *Xenopus* development, the germline is generated by inheritance of specialized cytoplasm called 'germ plasm'. Germ plasm is present in the vegetal cortex of a fertilized egg, where it divides into about four blastomeres via the first two cleavages, and then distributes unequally to daughter cells until midblastula transition (MBT) (Taguchi *et al.*, 2012; Whittington and Dixon, 1975). Early in gastrulation (stage 10), germ plasm translocates from the cortex to the perinuclear region in primordial germ cells (PGCs) and divides equally into two daughter PGCs in later cell divisions. The germ plasm contains electron dense granules, many mitochondria, and specific mRNAs and proteins. Recently, we demonstrated that germ plasm contains determinants that are necessary and sufficient for germline specification (Tada *et al.*, 2012). To understand the mechanisms underlying germline specification in *Xenopus*, many RNA components of the germ plasm have been identified (Cuykendall and Houston, 2010; King *et al.*, 2005), including *Germes* mRNA (Berekelya *et al.*, 2003). The *Germes* gene is specifically expressed in the ovary. *Germes* mRNA has been detected in the entire cytoplasm of stage I oocytes and in the mitochondrial cloud of stage II oocytes. It is associated with the germ plasm until gastrulation and disappears after translocation to the perinuclear region. *Germes* encodes a protein with two leucine zipper motifs and an EF-hand motif (Berekelya *et al.*, 2003). It has been shown that *Germes* protein also localizes to the germ plasm by expression of EGFP-tagged *Germes* protein in oocytes (Berekelya *et al.*, 2007). A reduction in the number of PGCs has been observed in tailbud (stage 31–33) embryos overexpressing

intact *Germes* (*Germes*^{WT}) or *Germes* lacking both leucine zipper motifs (*Germes*^{ΔLZs}). Interestingly, in these tailbud embryos, some PGCs are larger and found inside the endodermal mass, indicating that active PGC migration is blocked from an early stage. Using *Xpat* mRNA and its protein as a germ plasm marker (Hudson and Woodland, 1998), it has been revealed that the germ plasm at stage 31–33 has a morphology similar to that at earlier stages. In addition, it has been shown that *Germes* protein interacts with dynein light chain 8 *in vitro* and *in vivo* (Berekelya *et al.*, 2007). These findings suggest that *Germes* is involved in PGC migration and germ plasm organization.

The *DEADSouth* gene encodes DEAD-box RNA helicase belonging to the DDX25 family, and its transcript has also been identified as an RNA component of the germ plasm in *Xenopus* (MacArthur *et al.*, 2000). Recently, we generated transgenic *Xenopus* expressing EGFP fused with a mitochondrial targeting signal (mito-EGFP) for observation of the germ plasm in living embryos (Taguchi *et al.*, 2012), because germ plasm is enriched with mitochondria (Venkatarama *et al.*, 2010; Elinson *et al.*, 2011). Using mito-EGFP embryos, we demonstrated that *DEADSouth* protein localizes to the germ plasm, where it is required for proper PGC development (Yamaguchi *et al.*, 2013). Interestingly, knockdown of *DEADSouth* mRNA causes expansion of the germ plasm, inhibition of germ plasm translocation and division of PGCs after MBT. As a result, a reduc-

Abbreviations used in this paper: MBT, midblastula transition.

*Address correspondence to: Takeshi Yamaguchi. Division of Morphogenesis, National Institute for Basic Biology, 38 Nishigonaka, Myodaiji, Okazaki, Aichi 444-8585, Japan. Tel/Fax: +81-564-55-7572. E-mail: ytakeshi@nibb.ac.jp or Hidefumi Orii. Department of Life Science, University of Hyogo, 3-2-1 Koto, Kamigori, Akou-gun, Hyogo 678-1297, Japan. Tel/Fax: +81-791-58-0187. E-mail: orii@sci.u-hyogo.ac.jp

Accepted: 17th April 2013. Final, author-corrected PDF published online: 3 July 2013. Edited by: Sally Dunwoodie

tion in the number of PGCs is observed in tailbud-stage embryos. The phenotype of *DEADSouth*-knockdown embryos is similar to that of embryos overexpressing *GermesWT* or *GermesΔLZs*. To understand the mechanisms underlying germ plasm organization, it is important to investigate the phenotypes of embryos overexpressing *GermesWT* or *GermesΔLZs* for comparison with those of *DEADSouth*-knockdown embryos, particularly at stages 7–12 that are much earlier than the tailbud stage. Although it has been very difficult to directly observe the germ plasm in isolated PGCs, the use of mito-EGFP *Xenopus* enables such observations (Taguchi et al., 2012; Yamaguchi et al., 2013). Here, we demonstrate that translocation of the germ plasm is inhibited by overexpression of *GermesWT* or *GermesΔLZs*, and by knockdown of *DEADSouth*, suggesting that both *Germes* and *DEADSouth* proteins are involved in the translocation of germ plasm during MBT.

Results and Discussion

To investigate the function of *Germes* in PGC development, we generated three constructs, including intact *Germes* (*GermesWT-DS*), *Germes* lacking the EF-hand motif (*GermesΔEFh-DS*), and *Germes* lacking both leucine zipper motifs (*GermesΔLZs-DS*) according to Berekelya et al. (2007). To ensure PGC-specific expression, the open reading frames (ORFs) were followed by the 3' untranslated region (UTR) of the *DEADSouth* gene that is expressed in a PGC-specific manner (Kataoka et al., 2006). Each mRNA (460 pg) was co-injected into the vegetal pole of a fertilized egg with *Venus-DEADSouth* 3' UTR mRNA (*v-DS*, 460 pg) as a PGC tracer (Kataoka et al., 2006). At stage 32, significantly reduced numbers of PGCs were observed in embryos injected with *GermesWT-DS* or *GermesΔLZs-DS*, compared with those injected with only *v-DS* (*GermesWT-DS*, 9.2 ± 3.2 ; *GermesΔLZs-DS*, 10.5 ± 3.5 ; and *v-DS*, 17.9 ± 2.6) (Fig. 1 A–C,F). Embryos injected with 460 pg *GermesΔEFh-DS* mRNA showed no reduction in PGC

numbers (16.1 ± 2.9) (Fig. 1 D,F). These effects were identical to those described in a previous report in which PGCs were visualized by whole-mount *in situ* hybridization using the PGC-specific gene *Xpat* (Berekelya et al., 2007). Furthermore, we examined the effect of *GermesΔEFh-DS* when twice the amount of mRNA (920 pg/embryo) was injected. Interestingly, *GermesΔEFh-DS* also resulted in a significant reduction of PGC numbers (8.9 ± 1.9) (Fig. 1 E,F), although the injected embryos developed normally. This result indicated that overexpression of *GermesWT-DS*, *GermesΔLZs-DS*, and *GermesΔEFh-DS* resulted in similar reductions of PGC numbers, but are different in terms of the magnitude of their effect. These differences might have occurred because *Germes* functions are regulated by multiple domains (see below).

Next, we used embryos from transgenic *Xenopus* expressing EGFP with the mitochondrial targeting signal (mito-EGFP) to examine the effects caused by overexpression of *Germes-DS* and *Germes* mutants. At stage 12, a significant reduction of PGC numbers was observed in mito-EGFP embryos injected with *GermesWT-DS* (7.8 ± 0.7 , $P < 0.05$) or *GermesΔLZs-DS* (6.3 ± 1.9 , $P < 0.01$) mRNAs, compared with that in the control (11.0 ± 2.6). However, we did not observe significantly reduced PGC numbers in embryos injected with *GermesΔEFh-DS*, even at a dose of 920 pg/embryo (Fig. 1 G). We also investigated the size distribution of PGCs at stage 12 (Fig. 2). The average diameters of PGCs from mito-EGFP embryos injected with *GermesWT-DS* (460 pg/embryo), *GermesΔLZs-DS* (460 pg/embryo) or *GermesΔEFh-DS* (920 pg/embryo) were $59.6 \pm 24.4 \mu\text{m}$, $56.9 \pm 21.2 \mu\text{m}$ and $57.6 \pm 18.1 \mu\text{m}$, respectively. The diameters of these PGCs were significantly larger than those of control PGCs ($48.4 \pm 8.0 \mu\text{m}$). Moreover, these phenotypes were very similar to those of *DEADSouth* knockdown (Yamaguchi et al., 2013).

We also examined the morphology and intracellular localization of the germ plasm in PGCs from mito-EGFP embryos injected with *GermesWT-DS* or *Germes* mutant mRNAs. In uninjected PGCs,

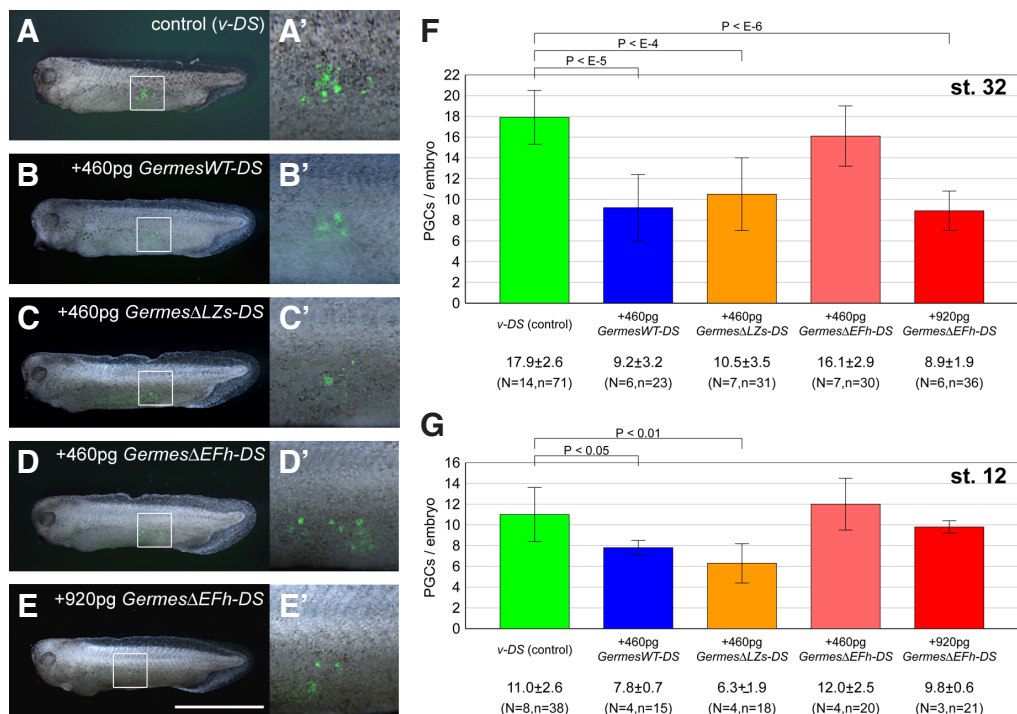
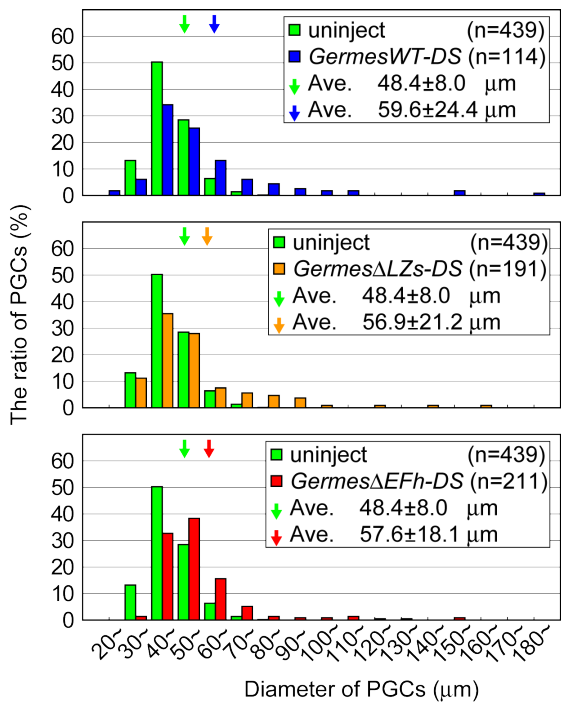


Fig. 1. Effect of overexpression of *GermesWT-DS*, *GermesΔLZs-DS* or *GermesΔEFh-DS* in PGCs. (A–E) Representative examples of tailbud embryos injected with mRNA of *v-DS* only, *v-DS* plus *GermesWT-DS*, *v-DS* plus *GermesΔLZs-DS*, or *GermesΔEFh-DS*, respectively. The amount of injected mRNA is indicated. Anterior is toward the left. Scale bar, 1 mm. (A'–E') High magnifications of the areas indicated in (A–E), respectively. (F) The number of PGCs per embryo at stage 32 injected with the indicated mRNAs. PGC numbers were determined by externally counting from both sides. (G) The number of PGCs per embryo at stage 12. Mito-EGFP transgenic embryos were injected with the indicated mRNAs, and then dissociated at stage 12. EGFP-positive and large cells were counted as PGCs. *N* and *n* indicate the number of experiments and total embryos examined, respectively. Error bars indicate standard deviation. One-tailed P-values were calculated by the Student t-test for significance.



the germ plasm was present in the cortex at stage 7, and then moved to the perinuclear region at stage 9. In embryos injected with *GermesWT-DS* or *Germes* mutants, many large PGCs, which retained the germ plasm in the cortex, were observed at stage 12

Fig. 2. Size distribution of PGCs from stage 12 embryos injected with *GermesWT-DS*, *GermesΔLZs-DS* or *GermesΔEFh-DS* mRNAs. PGCs were isolated from the injected mito-EGFP embryos to measure their diameter. Total numbers of isolated PGCs (*n*) are shown as 100%. The size distribution of PGCs in embryos injected with 460 pg *GermesWT-DS* (blue), 460 pg *GermesΔLZs-DS* (orange), or 920 pg *GermesΔEFh-DS* (red) is compared with that in uninjected embryos (green). *n* indicates total PGC numbers. Arrows indicate average diameters in the indicated experiments.

(Fig. 3A) in contrast to perinuclear localization of the germ plasm in most PGCs of uninjected embryos. Quantitative analysis demonstrated that 32.6%, 30.9% and 18.4% of PGCs in embryos injected with *GermesWT-DS*, *GermesΔLZs-DS* or *GermesΔEFh-DS* (920 pg), respectively, contained germ plasm in the cortex at stage 12, compared with only 6.8% of PGCs in uninjected embryos (Fig. 3B). These differences were significant ($P < 0.01$, *U*-test). Interestingly, we could not detect any alteration in the PGCs of injected embryos until stage 7. The mislocalization of germ plasm in these PGCs was very similar to that in *DEADSouth*-knockdown PGCs (Yamaguchi *et al.*, 2013). To elucidate the relationship among *Germes*, germ plasm translocation, and mitosis, we individually cultured PGCs isolated from stage 8 embryos injected with *GermesWT-DS*, and followed PGC mitosis for 11 hours (Fig. 4A). All five experiments (about 12 PGCs each/female/experiment) showed that mitosis of PGCs overexpressing *GermesWT-DS* was significantly inhibited compared with that in the control ($35.7 \pm 21.7\%$ vs. $46.3 \pm 20.4\%$; $P < 0.05$, paired samples *t*-test). Interestingly, in non-dividing PGCs, mislocalization of germ plasm was observed more frequently in

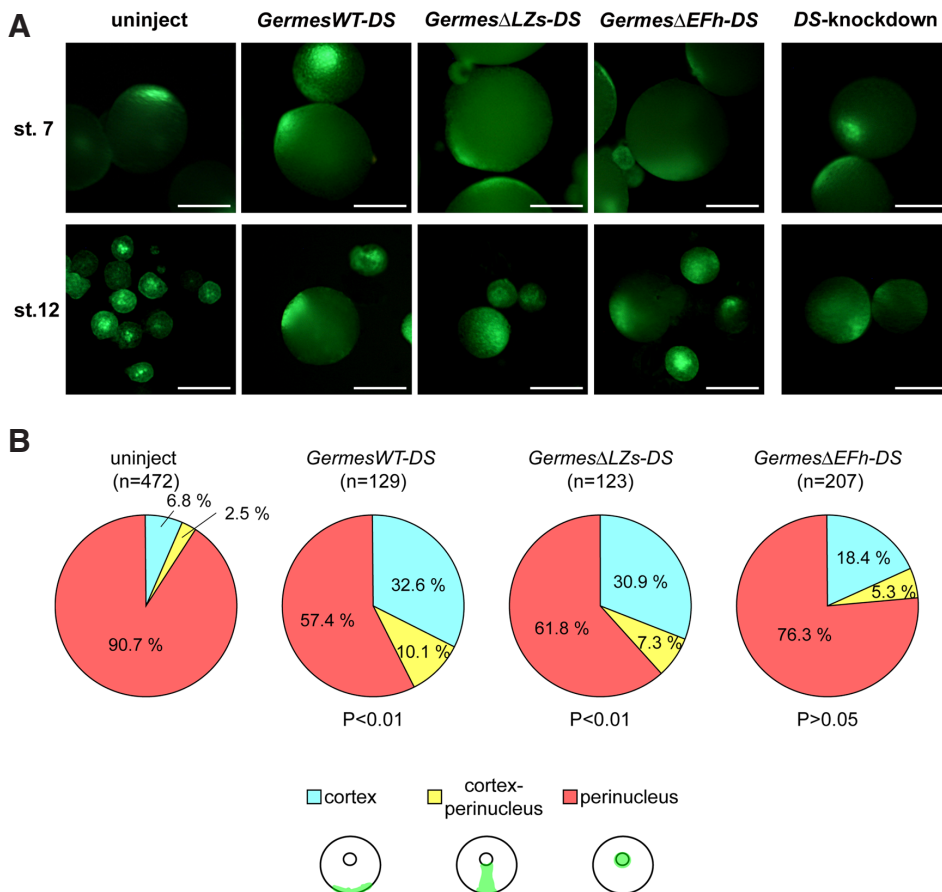


Fig. 3. Overexpression of *GermesWT-DS*, *GermesΔLZs-DS*, or *GermesΔEFh-DS* affects translocation of the germ plasm. (A) Localization of the germ plasm in PGCs isolated from mito-EGFP embryos at stages 7 (upper) and 12 (lower), which were injected with *GermesWT-DS* (460 pg), *GermesΔLZs-DS* (460 pg) or *GermesΔEFh-DS* (920 pg) mRNAs. For comparison, PGCs from uninjected and *DEADSouth*-knockdown (DS-knockdown; Yamaguchi *et al.*, 2013) embryos are also shown. The images represent the severe phenotypes of PGCs in the experiment. Scale bars, 100 μm. Note that, at stage 12, PGCs overexpressing *GermesWT-DS*, *GermesΔLZs-DS*, or *GermesΔEFh-DS*, and DS-knockdown PGCs are relatively large and contain the germ plasm beneath the cell membrane. (B) Ratio of PGCs with three localization patterns of germ plasm from stage 12 embryos uninjected or injected with *GermesWT-DS* (460 pg), *GermesΔLZs-DS* (460 pg) or *GermesΔEFh-DS* (920 pg) mRNAs. According to the localization patterns, PGCs were classified into three groups: cortex, perinucleus, and intermediate (cortex-perinucleus) as shown at the bottom of the panel. P-values were calculated by the Mann-Whitney U-test for significance.

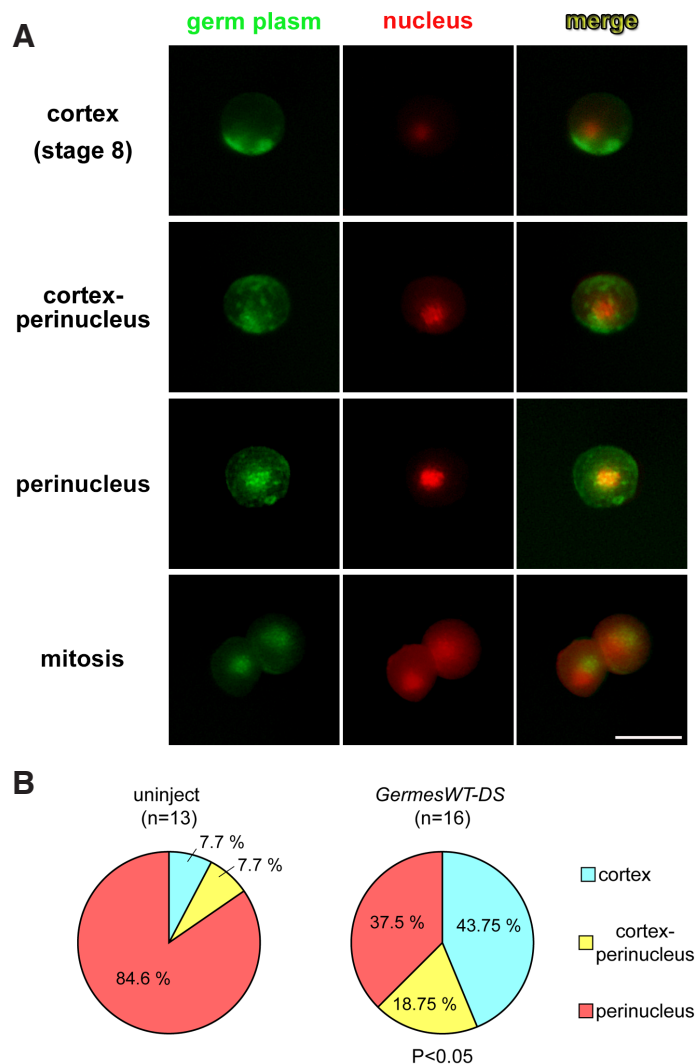


Fig. 4. Overexpression of *GermesWT-DS* results in mitotic inhibition of PGCs with mislocalized germ plasm. (A) Behavior of germ plasm (green) during mitosis of a single cultured PGC from normal mito-EGFP transgenic embryos at stage 8. Note that mitosis occurs after translocation of germ plasm from the cortex to the perinuclear region. Mitosis was observable at about 9 hours after isolation. Nuclei were labeled by injection of mCherry-NLS-DEADSouth 3' UTR mRNA (red). (B) Ratio of non-divided PGCs with three localization patterns of germ plasm after culture. The PGCs from stage-8 embryos uninjected or injected with *GermesWT-DS* (460 pg) were cultured individually for 11 hours. Classification of non-divided PGCs and statistical analysis were performed as described in Fig. 3. Scale bar, 100 μ m.

PGCs overexpressing *GermesWT-DS* than that in control PGCs (Fig. 4B). This difference was also significant ($P < 0.05$, U-test). Conversely, perinuclear localization of the germ plasm was observed in all divided PGCs in control and overexpression of *GermesWT-DS*. Translocation of the germ plasm occurred prior to the initial equal division of PGCs after MBT. Taken together, these observations strongly suggested that abnormal translocation of germ plasm by overexpression of *GermesWT-DS* or *Germes* mutants resulted in inhibition of equal division of PGCs. It was likely that these large PGCs could not move normally in the endodermal mass as described previously (Berekelya et al., 2007). Based on observations

of the PGCs from tailbud embryos (at stage 31–33) injected with *GermesWT* or *Germes Δ LZs* mRNAs, Berekelya et al., (2007) suggested that *Germes* is involved in the organization and functioning of germ plasm. In their study, it was unclear why overexpression of *Germes Δ EFh* caused no phenotypic effects, because the EF-hand domain is thought to bind calcium ions to regulate physiological roles. Here, we demonstrated that overexpression of *Germes Δ EFh* also caused phenotypic effects similar to those of *GermesWT* or *Germes Δ LZs* overexpression. The effects of their overexpression might be caused by competition for multiple *Germes*-interacting proteins including dynein light chain 8 (Berekelya et al., 2007).

Recently, we showed that translocation of the germ plasm is sensitive to nocodazole, but insensitive to cytochalasin D, and that α -tubulin is co-localized with germ plasm (Taguchi et al., 2012). These findings indicate that germ plasm translocates from the cortex to the perinuclear region through the microtubule system, but not the microfilament system. This observation is in good agreement with that of *Germes* protein interacting with dynein light chain 8 *in vitro* and *in vivo* (Berekelya et al., 2007). Germ plasm may be transported along microtubules to the perinuclear region by a dynein motor. However, the directionality of microtubules for germ plasm translocation remains to be determined.

It is very interesting that the phenotypes caused by overexpression of *GermesWT*, *Germes Δ LZs*, or *Germes Δ EFh* were very similar to those of *DEADSouth*-depleted embryos. Because *DEADSouth* is an RNA helicase with some similarity to eIF4A, it may be involved in translation of germ plasm-specific mRNAs (MacArthur et al., 2000). The subcellular region-specific translation of such mRNAs may be coupled to germ plasm translocation with *Germes*. Although we have not determined whether *Germes* associates with *DEADSouth* directly or indirectly, both proteins are obviously indispensable for proper maintenance and translocation of the germ plasm. After translocation, interactions between the germ plasm and nucleus would be required for germline specification. To understand the mechanisms underlying germline specification, it would be necessary to delineate more components of the germ plasm and their interactions with each other.

Materials and Methods

Xenopus embryos

Eggs and embryos from wild-type *Xenopus laevis* were prepared as described previously (Kataoka et al., 2006). Female transgenic *Xenopus laevis* expressing EGFP fused with a mitochondrial targeting signal (mito-EGFP) were also used in this study (Taguchi et al., 2012; Yamaguchi et al., 2013).

Preparation of constructs

The *Germes* ORF was amplified by a nested PCR method using ovarian cDNA from *Xenopus laevis* as a template, and was exchanged for the *Venus* ORF of pCS2-Venus-DEADSouth 3' UTR (pCS2-*Germes*-DEADSouth 3' UTR). For the initial amplification, the sequences of the forward and reverse primers were CCTGTGACTCCTATATATGTGCTGGAACAT and CAAGTTTGGCATGTACAAGGTATACTCTGG, respectively. The PCR product was subjected to a secondary amplification using the nested forward and reverse primers, CTTTTTGCAGGATCCATGTGGCAAATGCTGAAATATGTGGT and CTCATCACTGAATTCCTTAAGTATGGCTTAATTTTTGCGCCCT, respectively (sequences overlapping with the pCS2-Venus-DEADSouth 3' UTR are underlined). pCS2-*Germes Δ LZs*-DEADSouth 3' UTR and pCS2-*Germes Δ EFh*-DEADSouth 3' UTR constructs were generated by inverse PCR and In-Fusion technology (Clontech) using pCS2-*Germes*-

DEADSouth 3'UTR as a template. The amino acid sequences of GermesWT, Germes Δ LZs and Germes Δ EFh used in this study were identical to those in a previous report by Berekelya *et al.*, (2007).

Preparation and microinjection of mRNA

Template plasmids were linearized by digestion with *NotI* and used as templates for *in vitro* mRNA synthesis with an mMESSAGE mMACHINE SP6 kit (Ambion). The mRNA was microinjected into the cortical region at the vegetal pole of a fertilized egg with a Nonoject II microinjector (Drummond Scientific Company). Each mRNA (460 pg, 4.6 nL of 100 ng/ μ L mRNA) was injected into a fertilized egg. The same amount of *v-DS* mRNA was co-injected as a PGC tracer.

Observation of PGCs and germ plasm

PGCs were observed and counted externally in *v-DS*-co-injected embryos at stage 32 (Kataoka *et al.*, 2006). The PGCs were also isolated manually from dissociated transgenic embryos, counted, and examined for intracellular localization of the germ plasm (Yamaguchi *et al.*, 2013). PGCs from stage 8-transgenic embryos were uninjected or injected with 460 pg *GermesWT-DS*mRNA, and then individually seeded on 1% agarose-coated dishes containing 55% Leibovitz's L-15 medium (Gibco) supplemented with 5% fetal bovine serum, and then cultured at 25 °C for 11 hours. Germ plasm behavior was observed in PGCs from embryos injected with 460 pg *mCherry-NLS* (SV40 nuclear localization signal)-*DEADSouth* 3' UTR mRNA for nuclear staining (Taguchi *et al.*, in preparation).

Acknowledgements

We thank the members of our laboratory, and particularly Dr. Makoto Mochii, for their support.

References

BEREKELYA, L.A., PONOMAREV, M.B., LUCHINSKAYA, N.N., BELYAVSKY, A.V. (2003). *Xenopus* Germes encodes a novel germ plasm-associated transcript. *Gene Expr. Patterns* 3: 521-524.

BEREKELYA, L.A., MIKRYUKOV, A.A., LUCHINSKAYA, N.N., PONOMAREV, M.B., WOODLAND, H.R., BELYAVSKY, A.V. (2007). The protein encoded by the germ plasm RNA *Germes* associates with dynein light chains and functions in *Xenopus* germline development. *Differentiation* 75: 546-558.

CUYKENDALL, T.N., HOUSTON, D.W. (2010). Identification of germ plasm-associated transcripts by microarray analysis of *Xenopus* vegetal cortex RNA. *Dev. Dyn.* 239: 1838-1848.

ELINSON, R.P., SABO, M.C., FISHER, C., YAMAGUCHI, T., ORII, H., NATH, K. (2011). Germ plasm in *Eleutherodactylus coqui*, a direct developing frog with large eggs. *EvoDevo* 2: 20.

HUDSON, C., WOODLAND, H.R. (1998). *Xpat*, a gene expressed specifically in germ plasm and primordial germ cells of *Xenopus*. *Mech. Dev.* 73: 159-168.

KATAOKA, K., YAMAGUCHI, T., ORII, H., TAZAKI, A., WATANABE, K., MOCHII, M. (2006). Visualization of the *Xenopus* primordial germ cells using a green fluorescent protein controlled by *cis* elements of the 3' untranslated region of *DEADSouth* gene. *Mech. Dev.* 123: 746-760.

KING, M.L., MESSITT, T.J., MOWRY, K.L. (2005). Putting RNAs in the right place at the right time: RNA localization in the frog oocytes. *Biol. Cell* 97: 19-33.

MACARTHUR, H., HOUSTON, D.W., BUBUNENKO, M., MOSQUERA, L., KING, M.L. (2000). *DEADSouth* is a germ plasm specific DEAD-box RNA helicase in *Xenopus* related to eIF4A. *Mech. Dev.* 95: 291-295.

TADA, H., ORII, H., MOCHII, M., WATANABE, K. (2012). Ectopic formation of primordial germ cells by transplantation of the germ plasm: direct evidence for germ cell determinant in *Xenopus*. *Dev. Biol.* 371: 86-93.

TAGUCHI, A., TAKII, M., MOTOISHI, M., ORII, H., MOCHII, M., WATANABE, K. (2012). Analysis of localization and reorganization of germ plasm in *Xenopus* transgenic line with fluorescence-labeled mitochondria. *Dev. Growth Differ.* 54: 767-776.

VENKATARAMA, T., LAI, F., LUO, X., ZHOU, Y., NEWMAN, K., KING, M.L. (2010). Repression of zygotic gene expression in the *Xenopus* germline. *Development* 137: 651-660.

WHITINGTON, P.M., DIXON, K.E. (1975). Quantitative studies of germ plasm and germ cells during early embryogenesis of *Xenopus laevis*. *J. Embryol. Exp. Morph.* 33: 57-74.

YAMAGUCHI, T., TAGUCHI, A., WATANABE, K., ORII, H. (2013). *DEADSouth* protein localizes to germplasm and is required for the development of primordial germ cells in *Xenopus laevis*. *Biol. Open* 2: 191-199.

Further Related Reading, published previously in the *Int. J. Dev. Biol.*

Natural and artificial routes to pluripotency

Winfried H. Krueger, Lindsey C. Swanson, Borko Tanasijevic and Theodore P. Rasmussen
Int. J. Dev. Biol. (2010) 54: 1545-1564

Maternal RNAs encoding transcription factors for germline-specific gene expression in *Drosophila* embryos

Jun Yatsu, Makoto Hayashi, Masanori Mukai, Kayo Arita, Shuji Shigenobu and Satoru Kobayashi
Int. J. Dev. Biol. (2008) 52: 913-923

The formation of primordial germ cells from germline cells in spherical embryos derived from the blastodisc of 2-cell embryos in goldfish, *Carassius auratus*

Satoshi Otani, Tomoe Kitauchi, Taiju Saito, Suzu Sakao, Shingo Maegawa, Kunio Inoue, Katsutoshi Arai and Etsuro Yamaha
Int. J. Dev. Biol. (2005) 49: 843-850

Primordial germ cell migration

Kathleen Molyneaux and Christopher Wylie
Int. J. Dev. Biol. (2004) 48: 537-543

Primordial germ cell development: is the urodele pattern closer to mammals than to anurans?

M Wakahara
Int. J. Dev. Biol. (1996) 40: 653-659

5 yr ISI Impact Factor (2011) = 2.959

